

# Study of Insert Flank Wear and Surface Roughness Evolutions During Turning of Stellite 6 Based on RSM and Desirability Approaches

Riadh SAIDI\*, Tarek MABROUKI\*, Brahim BEN FATHALLAH\*,\*\*, Salim BELHADI\*\*\*, Mohamed Athmene YALLESE\*\*\*

\*University of Tunis El Manar, ENIT, Applied Mechanics and Engineering Laboratory (LR-11-ES19), BP 37 Le Belvédère 1002, E-mails: riadh.saidi@enit.utm.tn, tarek.mabrouki@enit.utm.tn

\*\*University of Tunis, ENSIT, Mechanical, Material and Process Laboratory (LR99ES05), 5 AV Taha Hussein Montfleury, Tunis, Tunisia, E-mail: brahim.benfathallah@enit.utm.tn

\*\*\*Mechanics and Structures Research Laboratory (LMS), May 8th 1945 University, P.O. Box 401, 24000 Guelma, Algeria, E-mails: belhadi23@yahoo.fr, yallese.m@gmail.com

<https://doi.org/10.5755/j02.mech.40674>

## Nomenclature

$V_c$  is a cutting speed (m/min);  $r$  is a tool tip radii (mm);  $ap$  is a cutting depth (mm);  $f$  is a feed rate (mm/rev); ANN is an artificial neural network; RSM is a response surface methodology; HRC is rockwell hardness; ANOVA is analysis of variance;  $DF$  is a desirability function;  $F$  value is a ratio of mean square of regression model;  $SC$  is a sum of squares;  $SS$  is a sequential sum of squares;  $MS$  is a mean squares;  $p$  value is a probability value;  $\alpha$  is a clearance angle (degree);  $\gamma$  is a rake angle (degree);  $\lambda$  is an inclination angle (degree);  $\chi_r$  is a cutting edge angle (degree);  $Ra$  is an arithmetic mean roughness ( $\mu\text{m}$ );  $VB$  is a tool flank wear (mm);  $R^2$  is a determination coefficient (%); Co-Cr-W alloy is Stellite 6.

## 1. Introduction

Applications in the aviation field have evolved significantly due to the increasing passenger capacity and flight range. One of the key factors in this evolution has been the development of materials science for aeroengines. Typically, components of aeroengine systems are made of nickel-, titanium-, cobalt-, and iron-based alloys, depending on their mechanical and thermal requirements.

Cobalt alloys are widely used in the aerospace industry for applications requiring excellent mechanical strength at high temperatures. However, these alloys are also known to be difficult to machine. The main problems in relationship with dry machining of cobalt alloys are low material removal rates and limited tool life. The low thermal conductivity (about 15 W/m K) and the high chemical affinity for many materials often lead to the formation of a layer of adhesion on the surface of the tool, which causes premature wear of the tool [1].

Cobalt-based alloys are extensively used in the aerospace industry, accounting for approximately 75% of the weight in aerospace applications and 50% in modern jet engines. Co-Cr-Mo alloy Stellite 6 has a high strength-to-weight ratio, excellent resistance to elevated temperatures and creep, and outstanding corrosion resistance.

Furthermore, properties like high mechanical strength, fracture toughness, ductility, hardenability and low thermal conductivity may have a negative impact on machinability. To overcome the problems of poor machinability and reduced tool life, it is essential to find the optimum

combination of cutting strategies using the most appropriate insert.

Cobalt alloys are known for their hardness and toughness causing a bad machinability and an increasing in the production cost of fabricated parts.

Bagci and Aykut [2] improved the surface roughness by varying the cutting speed, feed rate, and depth of cut using the Taguchi optimization method. The tool used in all tests had a TiN coating, coated with PVD. The experiments were optimized with the parameters calculated for a reliability of 95%, and the measured roughness ( $Ra$ ) was 0.143  $\mu\text{m}$ .

Bagci and Aykut [2] conducted an analysis of tool wear, cutting forces, and chip morphology resulting from optimizations in cutting parameters. They performed ninety experiments with different cutting parameters, using both uncoated and PVD-coated carbide tools. Aykut et al. [3] optimized the values of cutting forces and workpiece roughness using different combinations of cutting speed, feed, and depth of cut, with uncoated carbide tools, aided by mathematical models. They found that the main factor influencing roughness was the feed.

Folea et al. [4] investigated the impact of cutting speed, feed, and depth of cut on the roughness of alloy FSX 414. Coated carbide tools (Ti PVD) were used with various combinations of cutting parameters, and the surface finish quality was measured after each pass. A statistical analysis was conducted to determine the effect of the parameters on the surface finish quality.

Shao et al. [5] investigated cobalt alloy Stellite 12 using coated and non-coated cutting tools with different cutting parameters. The inserts used were uncoated tungsten carbide inserts (YT726 and YG610) and a TiAlN-coated carbide insert (SNMG150612-SM1105). The study measured tool flank wear using an optical microscope. Inserts referenced YG610 showed less wear than those of YT726 for all cutting conditions tested. In uncoated tools, tool breakage was caused by the progression of flank wear. At high cutting speeds, diffusion and chemical wear were the dominant factors.

Chavoshi [6] utilised mathematical models to predict the roughness of a part by varying cutting parameters, using inserts coated with TiN by PVD. Experimental confirmation was then carried out to verify the consistency of the mathematical models. The results showed that the cutting speed and cutting depth were the parameters that most influenced tool wear.

Ozturk [7] investigated the influence of cutting parameters on roughness when machining the cobalt alloy Stellite 6 using two different cutting tools: ceramic reinforced with whisker and tungsten carbide. The cutting speed and feed were varied, and roughness was measured for each test. Theoretical values were calculated using the Taguchi methodology. Results showed that ceramic tools outperformed tungsten carbide tools for the same cutting parameters, with feed having the greatest influence on roughness.

Bordin et al. [8] conducted a study on the influence of cutting speed and feed on surface integrity during the cutting of ASTM F1537 alloy. They analyzed surface finish, subsurface microhardness, and residual stresses while varying process parameters. The cutting time was established as three minutes. The study revealed that the feed rate was the primary factor affecting the roughness of the surface. It was observed that the smoothest surface was achieved with the lowest feed rate. Additionally, the lowest roughness was observed with the highest cutting speed.

Sarikaya and Güllü [9] investigated the influence of cutting speed and coolant flow on mean roughness ( $R_a$ ) using minimum quantity lubrication (MQL) coolant and an uncoated carbide tool. Three different types of lubricants were tested: mineral oil, mineral oil with synthetic ester, and vegetable oil. Cutting speed and fluid flow were varied while maintaining a constant feed and depth of cut. The optimal combination for reducing tool wear and surface roughness was achieved by using vegetable-based cutting fluid at maximum flow rate and minimum cutting speed.

Sarikaya and Güllü [10] investigated the effect of cutting parameters on surface roughness using uncoated carbide inserts (SNMG 120408-QM). The  $R_a$  roughness analysis was performed under both dry and flood cooling conditions. The results showed that the lowest roughness values were achieved with medium cutting speed and minimum feed, while the use of coolant further improved the surface quality. However, at high cutting speeds, the roughness increased due to tool wear progression.

Sarikaya et al. [11] conducted an analysis of wear and roughness using three different lubrication-cooling methods: dry, flood cooling, and MQL. They varied cutting speed and feed while using the same insert class as in previous research. The MQL lubrication-cooling method yielded better results than the other methods. However, at very high or very low cutting speeds, there was an increase in roughness and tool wear. In general, the lowest roughness values were observed with the lowest feeds. After applying the Taguchi method for optimization, the ideal combination for achieving the lowest roughness was found to be the use of the MQL method, medium cutting speed, and low feed. To minimize tool wear, it is recommended to use the MQL method with minimum cutting speed and the highest feed.

Other authors, Yingfei et al. [12] investigated the impact of cutting parameters on tool wear, surface finish, residual stresses, and chip formation. The authors varied the cutting speed, feed rate, and depth of cut using carbide tools coated with TiAlN. To ensure consistency, they used a specific cutting length of 400 mm for each evaluation of tool wear and roughness values. The results showed that feed speed had the greatest influence on tool wear, accounting for 83% of the total. The primary wear mechanism observed was abrasion at low cutting speeds. For cutting speeds above 30 m/min, the most influential mechanisms were chipping,

diffusion, and breakage. The parameters that had the greatest impact on roughness were feed rate and cutting speed, accounting for 57% and 38% of the influence, respectively.

Saidi et al. [13], [14] investigated the impact of cutting parameters on the roughness of the part, cutting forces, and material removal rate (MRR). They utilized a carbide tool coated with physical vapor deposition (PVD) and tool tip radii of 0.2 mm, 0.4 mm, and 0.8 mm for various combinations of cutting parameters. To correlate the cutting parameters with the output variables, mathematical functions were defined based on initial measurements and numerical methods.

Rodriguez and Arrazola, [15] measured roughness and cutting forces using cryogenics. The cooling system was designed based on thermal analysis of the heat flow in the machining process. The project aimed to optimize the tool's geometry, which included a cavity to receive the cryogenic fluid ( $N_2$ ). The results showed a 12% reduction in cutting forces compared to other cryogenic cooling methods and a 15% reduction compared to dry cutting. Roughness values were reduced by 12% compared to tests using the unmodified insert. At average cutting speeds, there was a 25% reduction in roughness values.

Valíček et al. [16] conducted an analysis on the impact of cutting speed, feed, and depth of cut on the roughness of a part coated using the HVOF (high-velocity oxygen fuel) spray method. They used computational methods to define a mathematical equation that predicts roughness from various combinations of cutting parameters. The mathematical model indicates that feed has the greatest influence on roughness, followed by depth of cut and cutting speed. Studies have been conducted on the milling of cobalt alloys, specifically in the Stellite 6 alloy.

Andhare et al. [17] aimed to reduce output variables by adjusting input parameters using method MQL and tungsten carbide inserts with zirconium coating (TNMG160406UF). They tested twenty combinations of cutting speed, feed, and depth of cut. Statistical analysis of variance (ANOVA) was performed using Minitab 19 software to determine the significance of each input parameter on the measured variables. The optimal values of the cutoff parameters for a multivariate analysis were defined with the assistance of software.

Benghersallah et al. [18] conducted experimental tests with high cutting speeds using carbide inserts. They varied cutting speed, feed, and depth of cut to compare the values of cutting force and tool wear for multiple combinations of input parameters. The progressive flank wear was dominant in the tool, while in some tests with higher speeds, the presence of notch and chipping was observed.

For basic machining, the sustainability index and the quality of the operation depend on several parameters relating to the tooling, the workpiece and the cutting tool. These factors and parameters must be taken into account for a better cutting performance.

In the past, researchers have focused on fundamental approaches for machining improvement which can be summarized as following:

- ✓ the selection of optimal machining parameters [19],
- ✓ the use of advanced cooling and lubrication environments [20],
- ✓ the use of various types of coating technologies to extend tool life [21],

- ✓ the use of textured cutting tools to improve machining [22]
- ✓ and the modelling of the cutting environment to productively replicate experiments [23].

During modelling, software is used to observe the relationship between input and output parameters. This approach has several benefits, including reduced cost and time for the manager, operator and researcher. The best combinations of parameters to obtain responses within a desired range can be selected at the optimization stage. Thus, the consolidation of two basic methods is an effective approach in many ways.

This work highlights the effect of cutting parameters on surface roughness of workpieces and the evolution of tool wear. The aim of this study is to propose appropriate tools for turning operations on Stellite 6. To achieve this, a full factorial experimental design was employed. Main effect plots, iso-contours, and 3D plots were utilized to evaluate and discuss the obtained results. Additionally, the analysis of variance (ANOVA) method and Response Surface Methodology (RSM) were adopted to identify both reactive and non-reactive effects of experimental parameter responses.

## 2. Experimental Procedure

### 2.1. Workpiece material, cutting tool and experimental method

The material chosen for the workpiece in the current experiments was Co-Cr-Mo alloy Stellite 6, a high-strength alloy with a hardness of 41 HRC. The length and outer diameter of the work piece are 70 mm and 80 mm, respectively (Fig. 1). A cobalt alloy part specified Co-Cr-Mo alloy Stellite 6 was selected, which is preferable for biomedical and aerospace applications. The machining operations was carried out using lathe of the type SN 40C (with 6.6 kW spindle power of the Czech company "TOS TRENCIN"). The chemical composition of Co-Cr-Mo alloy Stellite 6 with all the percentages of elements is presented in Table 1.

To investigate the effect of cutting parameters on machined surface roughness and tool flank wear, we used carbide inserts with varying nose radii. In particular, the insert nose radii ( $r$ ) have been modified in three steps, 0.2 mm, 0.4 mm and 0.8 mm, optimal for turning the Co-Cr-Mo alloy Stellite 6. A PVD coated (Ti,Al)N insert was used. This has high hardness and oxidation resistance.

The turning process was based on the geometry of SANDVIK ISO Type CNGG and SGF 1105, which resulted in a better overall wear resistance. The tool holder is PCLNR 2020 K. Their geometry of the active part, as shown in Fig. 2, is the same for the following angles: cutting edge angle ( $\chi_r = +95^\circ$ ), inclination angle ( $\lambda = -6^\circ$ ), rake angle ( $\gamma = -6^\circ$ ), and clearance angle ( $\alpha = 0^\circ$ ), respectively.

The tests were conducted using three different feed rates ( $f$ ) of 0.08, 0.11, and 0.14 mm/rev, two cutting depths of 0.1 and 0.2 mm, and three cutting speeds of 85, 105, and 125 mm/mn. These values were selected based on the data sheets and recommendations of the tool manufacturers (SANDVIK Coromont).

### 2.2. Surface roughness ( $Ra$ ) measurement

By measuring Surftest SJ 201 along the feed direction, the surface finish ( $Ra$ ) of the machined surfaces at the end of each cut can be determined.

The instrument was equipped with a 2  $\mu$ m radius diamond stylus. A cut-off length ( $\lambda_c$ ) of 0.8 mm and an evaluation length of 4 mm were employed. The traverse speed was set at 0.5 mm/s, and a Gaussian filter according to ISO 4287 was applied. Measurements were performed along the feed direction. For each machined surface, three traces were acquired at uniformly distributed positions (at 120 degrees) along the machined track (Fig. 3). The reported  $Ra$  value corresponds to the mean of the three measurements. Calibration was performed prior to each test using a certified reference standard. The method ensured a repeatability of  $\pm 0.02 \mu$ m and an overall measurement uncertainty of  $\pm 5\%$ .

### 2.3. Tool flank wear (VB) measurement

A visual Gage 250 optical gauge microscope was utilized to observe the maximum cutting tool flank wear (VB).

Flank wear was assessed using a Visual Gage 250 optical microscope. Measurements were performed at 63,6x3 magnification, with an effective pixel size of 1.5  $\mu$ m/pixel. The system was calibrated with a certified calibration grid prior to measurements. Flank wear was defined and measured according to ISO 3685 as the average flank wear land width. The procedure consisted of image acquisition, edge detection, and digital measurement. For each tool, three measurements were taken at different locations along the cutting edge, and the reported VB value corresponds to the mean of these measurements. The methodology ensured a repeatability of  $\pm 2 \mu$ m and an overall measurement uncertainty of  $\pm 5\%$ .

### 2.4. Process modeling through RSM

Response Surface Methodology (RSM) is a statistical and mathematical technique used to develop, improve and optimise processes and is commonly used in industry where multiple input variables affect output variables.

The response surface methodology, also referred to as the polynomial regression model or the polynomial model, involves the construction and validation of the response function models. The response function models. Response surface methodology, also known as polynomial regression or polynomial model, involves constructing and validating response function models that can be used to search for optimal conditions.

This is known as indirect optimization. This is the process of defining a factor setting that best meets the stated response requirements when optimizing a response or finding a compromise among several responses. The modelling of a response surface is based on the analysis of the variation of the test results that are obtained according to a design of experiments.

RSM has been used to establish the mathematical models that combine the process results (surface roughness  $Ra$  and flank wear VB) with the four input parameters studied, such as cutting depth ( $ap$ ), cutting speed ( $V_c$ ), feed rate ( $f$ ) and tool nose radii ( $r$ ). The wear tests were carried out on 'Stellite 6' logs with a coated carbide tool (PVD,

GC1105) over a cutting length of 228 mm (in three passes). The experimental design is shown in Table 2, which also gives the values of ( $VB$ ) and ( $Ra$ ) obtained from measurements.

### 3. Results and Analysis

#### 3.1. Response Surface Methodology (RSM)

The first step in the determination of appropriate process parameters is the construction of mathematical

models of the process in order to establish a relationship between the inputs and outputs of the process. RSM is a popular statistical approach to establishing a specific relationship between a set of influencing input factors and a set of output measures [24].

In this work, BBD-based RSM models were used to show the mathematical relationships between the specified responses (cutting force, specific cutting energy and surface roughness) and a set of independent factors (speed, feed, depth of cut and cooling approaches), based on previous research by Zaman et Dhar [25].

Table 1

Chemical composition of the cobalt alloy stellite6, expressed in %, [12].

C	Mn	Si	P	S	Cr	W	Ni	Mo	Fe	Co
1.11	0.57	1.20	0.004	0.001	28.25	3.74	2.32	1.17	1.89	Balance

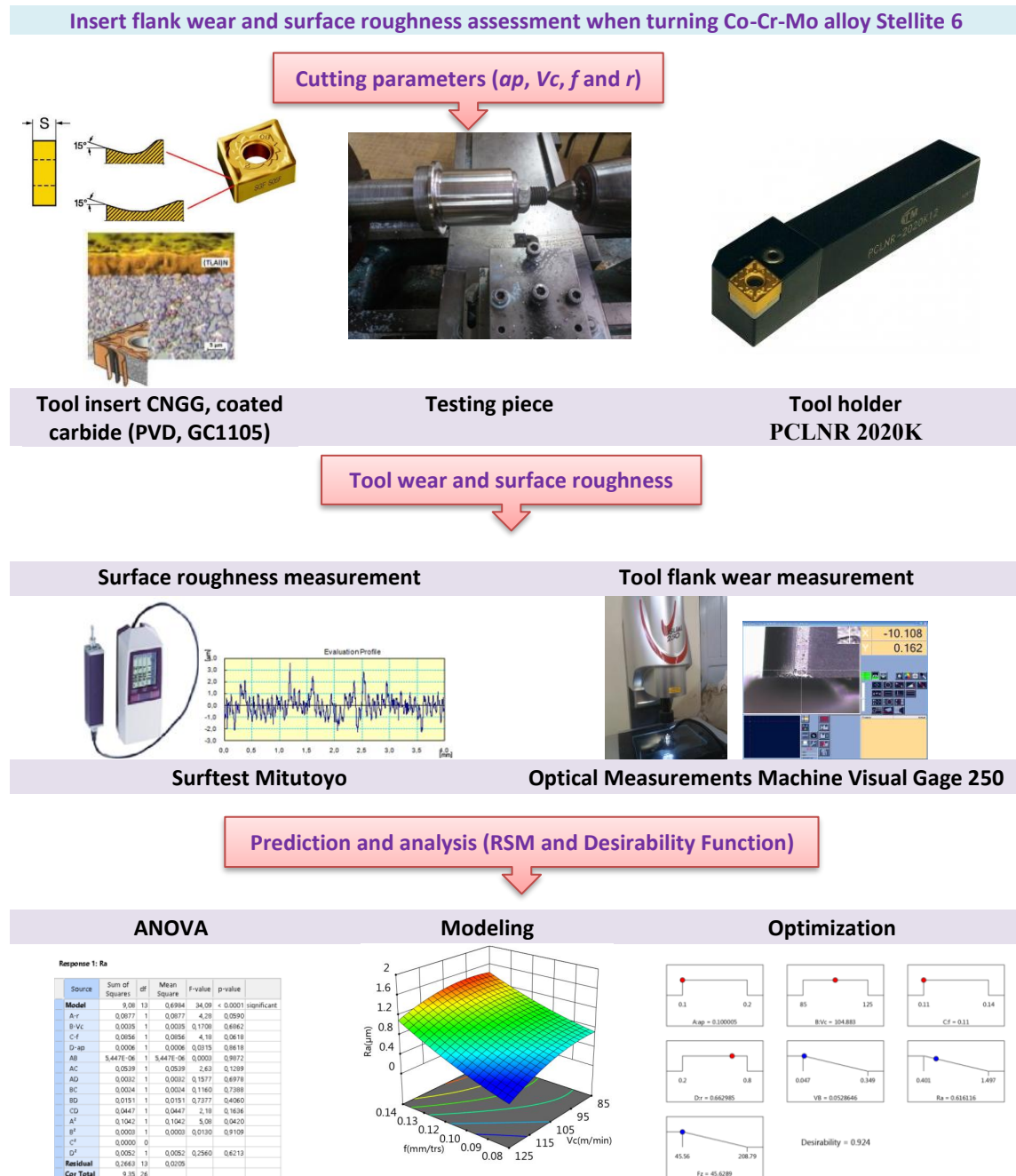


Fig. 1 The framework for research methodology

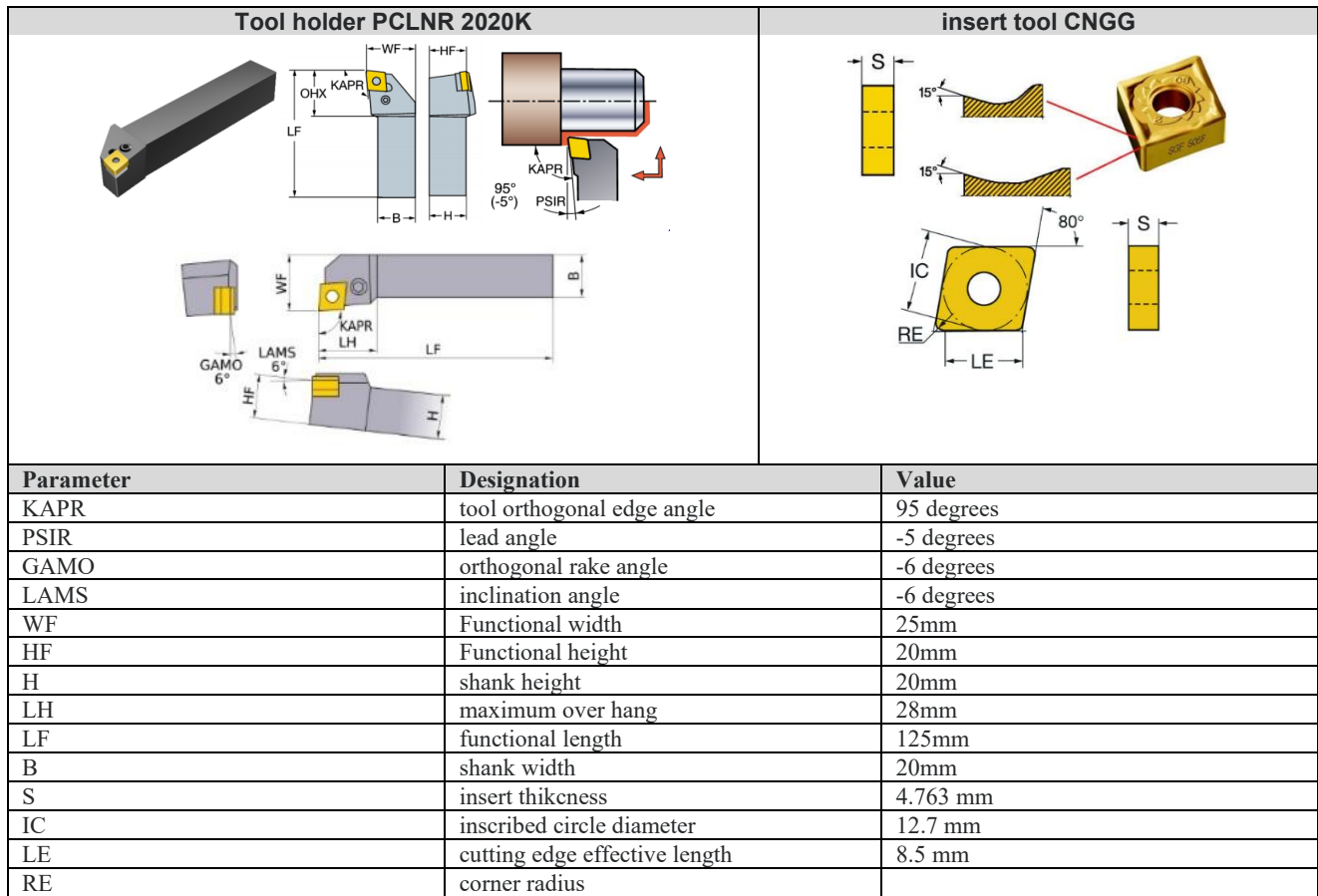


Fig. 2 Illustration of cutting tool geometry (SANDVIK Coromont)

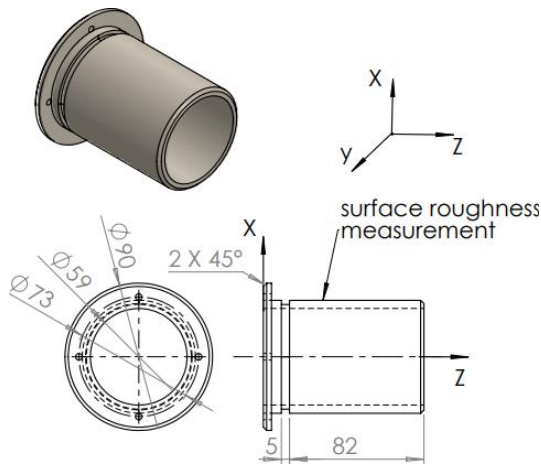


Fig. 3 Illustration of surface roughness measurement, performed three times along generatrices of the machined workpiece

Typically, a first-order polynomial is suitable for determining the main effects of individual input variables and for a relatively small region of independent variable space (low response curvature), whereas a second-order model can be used to determine the interaction effects of variables on output quality [26].

The mathematics of both first- and second-order models can be written symbolically as in Eq. (1)

$$Y = b_0 + \sum_{i=1}^n b_i X_i + \sum_{i,j} b_{ij} X_i X_j + \sum_{i=1}^n b_{ii} X_i^2 + \varepsilon, \quad (1)$$

where the term  $b_0$  is a constant, the regression coefficients;  $b_i$ ,  $b_{ii}$  and  $b_{ij}$  correspond to the linear, quadratic and interaction terms respectively. The coded variables  $X_i$  and  $X_j$  are associated with the process parameters ( $r$ ,  $V_c$ ,  $f$  and  $a_p$ ), parameter  $n$  is the number of factors and  $\varepsilon$  is a random error.

Table 2

## Experimental design

Run	Input variables				Output variables	
	$a_p$ , mm	$V_c$ , m/min	$f$ , mm/rev	$r$ , mm	$VB$ , mm	$Ra$ , $\mu$ m
1	0.1	85	0.08	0.2	0.076	0.65
2	0.1	85	0.11	0.4	0.063	0.74
3	0.1	85	0.14	0.8	0.094	0.97
4	0.1	105	0.08	0.4	0.081	0.6
5	0.1	105	0.11	0.8	0.075	0.46
6	0.1	105	0.14	0.2	0.047	1.58
7	0.1	125	0.08	0.2	0.08	0.48
8	0.1	125	0.11	0.4	0.082	0.61
9	0.1	125	0.14	0.8	0.111	0.93
10	0.2	85	0.08	0.8	0.105	0.8
11	0.2	85	0.11	0.2	0.09	0.88
12	0.2	85	0.14	0.4	0.111	1.23
13	0.2	105	0.08	0.8	0.063	0.56
14	0.2	105	0.11	0.2	0.106	0.85
15	0.2	105	0.14	0.4	0.102	1.15
16	0.2	125	0.08	0.4	0.100	0.4
17	0.2	125	0.11	0.8	0.148	0.62
18	0.2	125	0.14	0.2	0.349	0.74

The percentage contribution shown in the table (ANOVA) is expressed by Eq. (2):

$$\text{Contribution}(\%) = \text{SCM}/\text{SCT} \times 100. \quad (2)$$

The regression models are obtained using Design Expert software.

### 3.2. Statistical analysis

An ANOVA analysis was carried out at a significance level of  $\alpha = 0.05$ , corresponding to a 95% confidence level, to investigate the effect of cutting conditions on the evolution of insert wear ( $VB$ ).

The main objective is to study the effect of the cutting conditions ( $r$ ,  $V_c$ ,  $f$  and  $ap$ ) on the total variance of the results.

Table 3 shows the ANOVA results for surface roughness  $Ra$ . The analysis of variance shows that tool feed is the most significant parameter, followed by cutting speed and tool tip radii. Table 3 indicates that the contribution of feed rate, cutting speed and interaction ( $a_p \times r$ ) is 36.76%, 6.61% and 10.52% respectively.

$$\begin{aligned} Ra = & -2.85 + 10.2a_p + 0.0768V_c - 12.5f - 2.93r - 0.000387V_c \times V_c + 82f \times f - \\ & -0.58r \times r - 0.0694a_p \times V_c - 63.1a_p \times f + 11.21a_p \times r + 0.082V_c \times f - 0.0016V_c \times r + 14.6f \times r. \end{aligned} \quad (4)$$

The correlation of the  $VB$  wear criterion model is 96.26% (Eq. (5)).

$$\begin{aligned} VB = & 2.444 - 3.88a_p - 0.03586V_c - 9.64f + 0.772r + 0.000149V_c \times V_c + 22.8f \times f + \\ & + 0.341r \times r + 0.02305a_p \times V_c + 24.28a_p \times f - 2.162a_p \times r + 0.0332V_c \times f - 0.00236V_c \times r - 4.76f \times r. \end{aligned} \quad (5)$$

#### 3.2.2. Effects of cutting parameters on surface response factors

A comparison of the  $Ra$  values obtained from measurements and those predicted by the mathematical model Eq. (4) is shown in Fig. 4, a. The results show a good correlation.

The results of the  $VB$  values obtained from measurements and those predicted by the mathematical model (Eqs. (5)) are compared in Fig. 4, b.

On the basis of the results presented in Table 4, it can be concluded that the cutting speed ( $V_c$ ) is the most influential parameter with a contribution of 16.28% compared to the other parameters. This is followed by the depth of cut ( $ap$ ) (11.03%) and the tool tip radii (5.93%). Furthermore, with contributions of 12.00%, 8.55% and 12.28% respectively, the interactions ( $V_c \times V_c$ ), ( $a_p \times V_c$ ) and ( $a_p \times f$ ) have a significant influence on the evolution of the  $VB$  flank wear (Table 4)

#### 3.2.1. Regression equations

The correlation between the cutting conditions and the roughness ( $Ra$ ) and tool wear ( $VB$ ) measurements was translated into a quadratic regression using the Response Surface Methodology (RSM) approach. The regression equations in terms of real factors can be used to make predictions about the response for given levels of each factor. The correlation coefficient of the surface roughness ( $Ra$ ) model is 92.43% (Eq. (4)).

In fact, the correlation coefficient between the predicted and experimental surface roughness ( $Ra$ ) is 92.43%, while for flank wear ( $VB$ ) it reaches 96.26%, thus confirming a strong predictive accuracy of the developed models.

Table 5 displays the error values between the developed models and the experimental results for surface roughness and flank wear.

The response surface methodology can be used to provide a graphical representation of the effects of cutting

Table 3  
ANOVA results for surface roughness  $Ra$

Source	SS	DOF	Contribution, %	MS	F-value	p-value
Model	1.37	12	92.57	0.114	5.07	0.0425
$A-ap$	0.0064	1	0.43	0.006	0.2849	0.6164
$B-V_c$	0.0978	1	6.61	0.098	4.35	0.0913
$C-f$	0.544	1	36.76	0.544	24.23	0.0044
$D-r$	0.0168	1	1.14	0.017	0.746	0.4272
$AB$	0.0562	1	3.80	0.056	2.5	0.1746
$AC$	0.0613	1	4.14	0.061	2.73	0.1593
$AD$	0.1557	1	10.52	0.156	6.93	0.0464
$BC$	0.0113	1	0.76	0.011	0.5019	0.5103
$CD$	0.0407	1	2.75	0.041	1.81	0.2361
$B^2$	0.066	1	4.46	0.066	2.94	0.1471
$C^2$	0.0237	1	1.60	0.024	1.06	0.3513
$D^2$	0.0057	1	0.39	0.006	0.2555	0.6347
Residual	0.1123	5	7.59	0.023		
Cor Total	1.48	17	100			

Table 4  
ANOVA results for flank wear  $VB$

Source	SS	DOF	Contribution, %	MS	F-value	p-value
Model	0.07	13	96.28	0.005	7.91	0.0297
$A-ap$	0.008	1	11.03	0.008	11.82	0.0263
$B-V_c$	0.012	1	16.28	0.012	17.37	0.0141
$C-f$	0.004	1	5.66	0.004	6	0.0704
$D-r$	0.004	1	5.93	0.004	6.37	0.0651
$AB$	0.006	1	8.55	0.006	9.18	0.0388
$AC$	0.009	1	12.28	0.009	13.17	0.0222
$AD$	0.005	1	6.34	0.005	6.71	0.0607
$BC$	0.002	1	2.21	0.002	2.3	0.2043
$BD$	8E-04	1	1.10	8E-04	1.14	0.3465
$CD$	0.003	1	4.00	0.003	4.28	0.1074
$B^2$	0.009	1	12.00	0.009	12.9	0.0229
$C^2$	0.001	1	1.52	0.001	1.63	0.271
$D^2$	0.002	1	2.90	0.002	3.06	0.1554
Residual	0.003	4	3.72	7E-4		
Cor Total	0.073	17	100			

conditions on the response curves recorded during the cutting process of 'Stellite 6' over a cutting length of ( $L_c = 228$  mm).

In this way it is possible to visualise the importance of certain interaction effects on surface roughness ( $Ra$ ). Fig. 5, a shows that for the ( $a_p \times V_c$ ) interaction, increasing the depth of cut leads to the lowest roughness ( $Ra$ ).

The effect of the cutting speed is negligible. The surface and iso-contour plots in Fig. 5, b illustrate the effect

of the ( $f \times a_p$ ) interaction on the roughness  $Ra$  for  $V_c = 105$  m/min and  $r = 0.2$  mm. The results indicate that achieving minimum roughness  $Ra$  requires a simultaneous decrease in  $f$  and  $a_p$ . The effect of the cutting parameters  $V_c$  and  $f$  on the evolution of the roughness  $Ra$  for  $a_p = 0.2$  mm and  $r = 0.8$  mm is shown in Fig. 5, c. It can be seen that at low values of  $f$  the minimum roughness  $Ra$  is achieved.

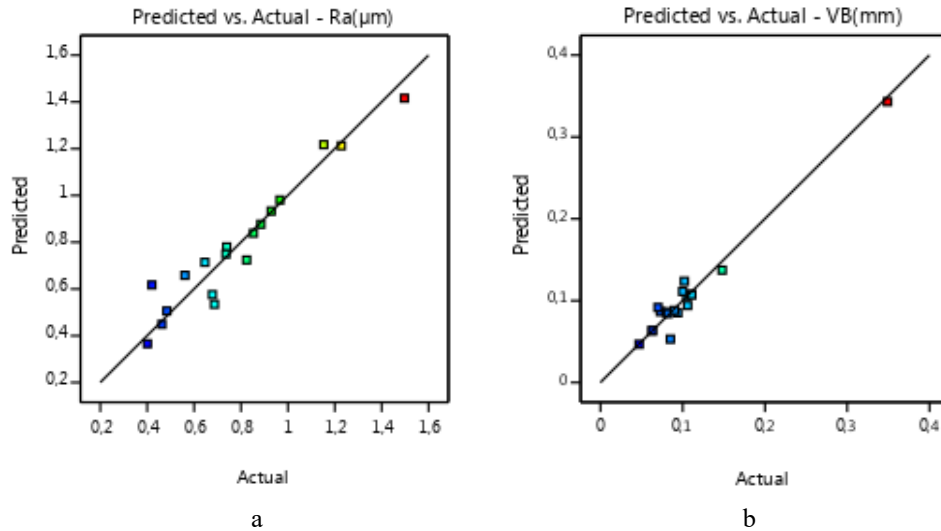


Fig. 4 Comparison between measured and predicted values a – surface roughness  $Ra$ , b – tool wear  $VB$

Table 5  
Error (%) between prediction and measurement of surface roughness and flank wear

Run	Measured		Predicted		Error, %	
	$Ra$ , $\mu m$	$VB$ , mm	$Ra$ , $\mu m$	$VB$ , mm	$Ra$	$VB$
1	0.65	0.076	0.71	0.087	9.88	13.82
2	0.74	0.063	0.78	0.064	5.42	0.79
3	0.97	0.094	0.98	0.085	1.07	9.36
4	0.6	0.081	0.53	0.073	10.90	9.75
5	0.46	0.075	0.45	0.079	2.39	5.33
6	1.58	0.047	1.42	0.047	10.13	0.43
7	0.48	0.08	0.51	0.086	5.42	7.88
8	0.61	0.082	0.66	0.084	7.97	2.56
9	0.93	0.111	0.93	0.108	0.33	2.88
10	0.8	0.105	0.72	0.106	9.50	0.48
11	0.88	0.09	0.88	0.088	0.35	2.11
12	1.23	0.111	1.21	0.107	1.63	3.42
13	0.56	0.063	0.62	0.063	10.23	0.63
14	0.85	0.106	0.84	0.094	1.35	11.13
15	1.15	0.102	1.22	0.114	6.09	11.57
16	0.4	0.1	0.37	0.111	8.53	11.30
17	0.62	0.148	0.58	0.137	7.10	7.23
18	0.74	0.349	0.75	0.343	1.27	1.66

The effect of  $V_c$  is negligible in this interaction.

The surface and iso-contour graphs (Fig. 5, d) demonstrate the effect of the ( $f \times r$ ) interaction on roughness  $Ra$  for  $a_p = 0.2$  mm and  $V_c = 85$  mm/min. The roughness  $Ra$  is minimal for small values of  $f$  and tool nose radii  $r$ .

Fig. 6, a shows that significant draft wear ( $VB$ ) is obtained for a simultaneous increase in cutting depth and cutting speed, for constant cutting conditions  $f = 0.14$  mm/rev and  $r = 0.2$  mm. This confirms the importance of the interaction ( $a_p \times V_c$ ) on wear evolution.

The surface and iso-contour plots (Fig. 6, b) show the effect of interaction ( $f \times a_p$ ) on wear ( $VB$ ) for  $V_c = 125$  m/min and  $r = 0.2$  mm. The results show that the increase in draft wear  $VB$  is associated with a simultaneous increase in  $f$  and  $a_p$ .

The graph in Fig. 6, c shows the effects of cutting parameters  $V_c$  and  $f$  on the evolution of wear  $VB$  for  $a_p = 0.2$  mm and  $r = 0.2$  mm. Here too, we can see that wear  $VB$  is significant, especially with a simultaneous increase in  $V_c$  and  $f$ . This shows the importance of the interaction effect ( $V_c \times f$ ).

Fig. 6, d shows the effects of cutting parameters  $V_c$  and  $r$  on the evolution of wear  $VB$  for  $a_p = 0.2$  mm and  $f = 0.14$  mm/rev. Here, we emphasize that minimum wear  $VB$  is only achieved when using low cutting speeds and high nose radii values simultaneously.

#### 4. Multi-Optimization of Machining Parameters with Desirability Function

Desirability Function ( $DF$ ) is not a direct method used to optimize [12]. It has been used to optimize several response factors ( $Ra$  and  $F_z$ ). Desirability function is a decision support tool used to identify process parameters that lead to close to optimum process response settings.

During the optimization process, the aim is to find the optimum values of the machining parameters in order to produce the lowest possible tool wear and to minimize the surface roughness ( $VB$  and  $Ra$ ).

Table 6 lists the objectives and parameter ranges for the optimization process. The RSM optimization results for  $VB$  and  $Ra$  are defined in Table 6 in order of decreasing desirability.



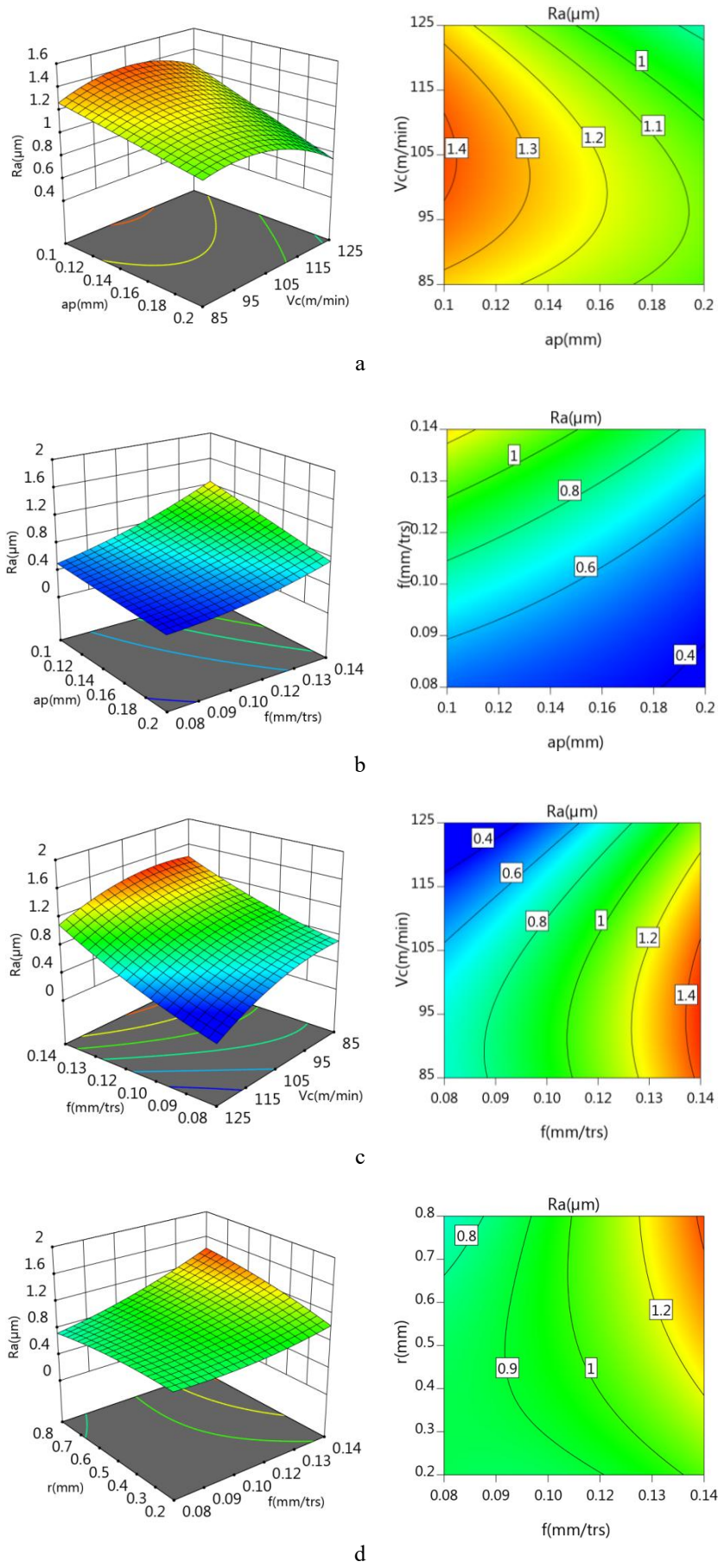


Fig. 5 Wear test results of effect of cutting conditions on the evolution of  $Ra$  ( $L_c = 228$  mm): a –  $f = 0.14$  mm/rev et  $r = 0.2$  mm, b –  $V_c = 105$  m/mn et  $r = 0.2$  mm, c –  $a_p = 0.2$  mm et  $r = 0.8$  mm, d –  $a_p = 0.2$  mm et  $V_c = 85$  mm/mn



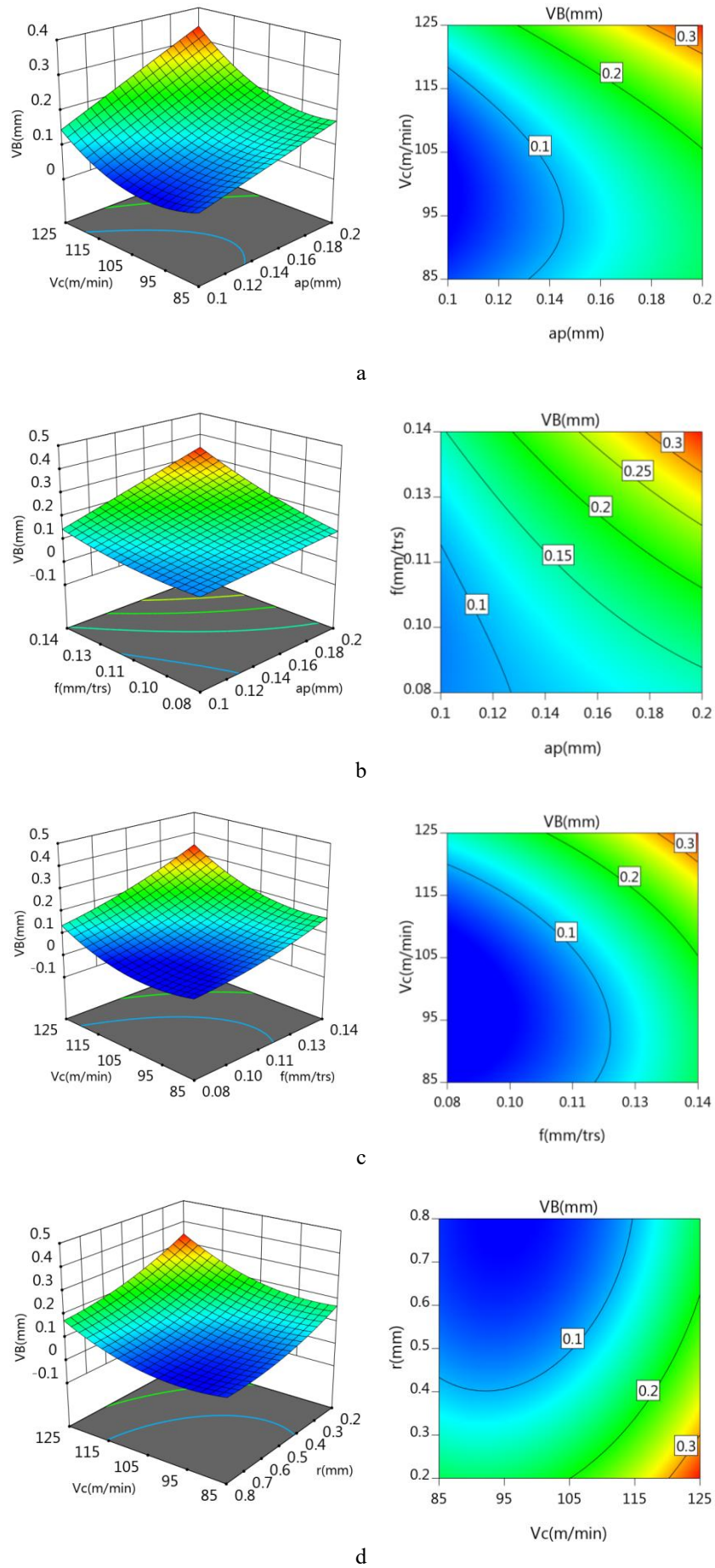


Fig. 6 Wear test results of effect of cutting conditions on the evolution of VB ( $L_c = 228$  mm): a –  $f = 0.14$  mm/rev et  $r = 0.2$  mm, b –  $V_c = 125$  m/mn et  $r = 0.2$  mm, c –  $a_p = 0.2$  mm et  $r = 0.2$  mm, d –  $a_p = 0.2$  mm et  $f = 0.14$  mm/rev

Table 6

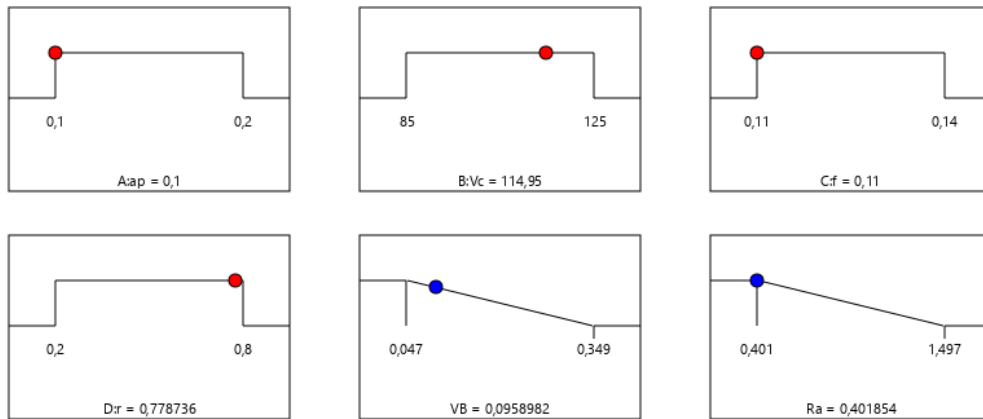
Goals and parameter ranges for optimization of cutting conditions

Name	Goal	Lower Limit	Upper Limit	Lower Weight	Upper Weight	Importance
$A:ap$	is in range	0.1	0.2	1	1	3
$B:Vc$	is in range	85	125	1	1	3
$C:f$	is in range	11	0.14	1	1	3
$D:r$	is in range	0.2	0.8	1	1	3
$VB$	minimize	0.047	0.349	1	1	5
$Ra$	minimize	0.401	1.497	1	1	5

Table 7

Response optimizations for tool wear and surface roughness parameters

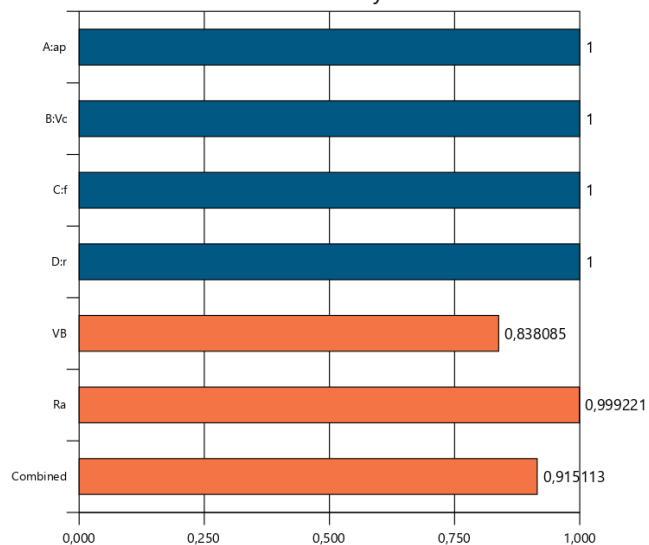
Number	$ap$	$Vc$	$f$	$r$	$VB$	$Ra$	Desirability	
1	0.100	114.950	0.110	0.779	0.096	0.402	0.915	Selected
2	0.100	114.600	0.110	0.782	0.096	0.401	0.915	
3	0.100	115.156	0.110	0.776	0.096	0.403	0.915	
4	0.100	114.958	0.110	0.774	0.094	0.408	0.915	
5	0.100	114.343	0.110	0.777	0.094	0.410	0.915	
6	0.100	115.836	0.110	0.771	0.096	0.401	0.915	
7	0.100	115.394	0.110	0.766	0.094	0.413	0.915	



Desirability = 0,915  
Solution 1 out of 100

a

Desirability



b

Fig. 7 Combined optimization of desirability for  $Ra$  and  $VB$ : a – ramp function graph, b – bar graph

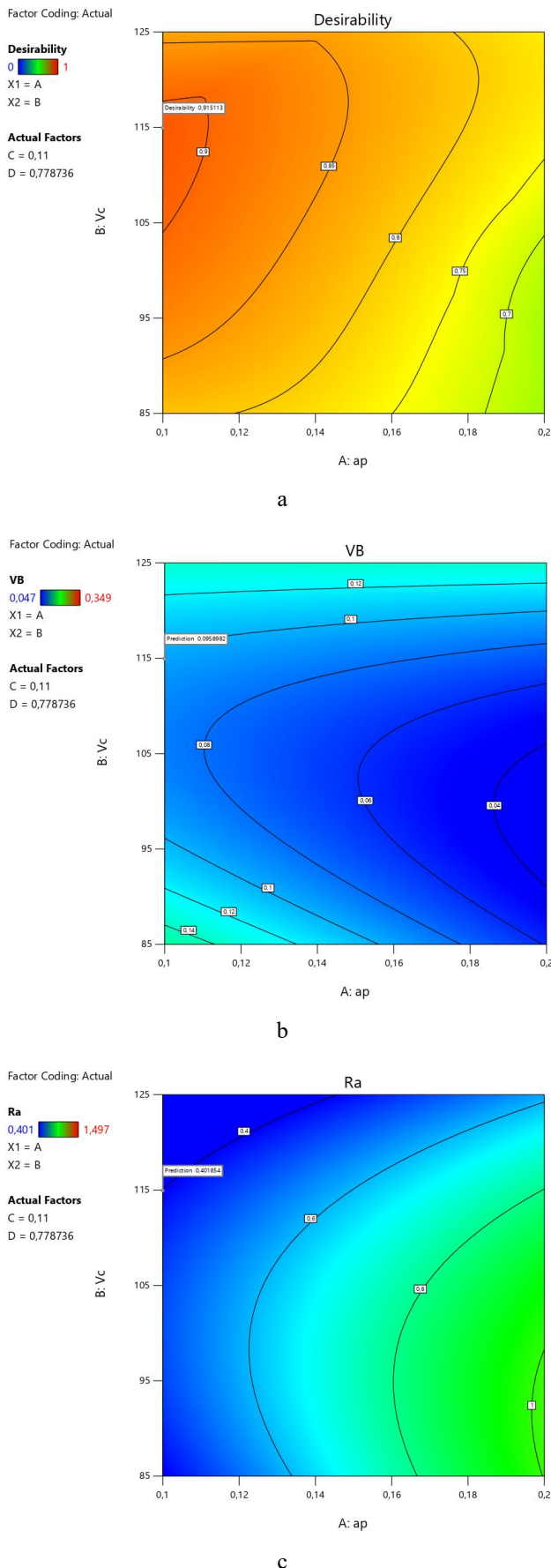


Fig. 7 Composite desirability for tool wear and surface roughness: a – desirability, b – tool wear, c – surface roughness

The Optimal results for tool wear  $VB$  and surface roughness  $Ra$  are 0.092 mm and 0.402  $\mu\text{m}$ , respectively.

The result of the combined desirability for these cutting conditions and responses is  $D = 0.915$  (Fig. 7, a and Fig. 7, b). Fig. 8 shows two-dimensional contour plots that explain the optimization results in terms of composite desirability (a), tool wear (b) and surface roughness (c).

## 5. Conclusions

This paper presents an investigation of the effect of cutting parameters on tool wear and surface roughness in the machining of a cobalt-based alloy, Stellite 6.

Using Response Surface Methodology (RSM), mathematical models were developed to define a relationship between input parameters (cutting speed, cutting time and tool hardness) and output variables. The analysis of variance (ANOVA) was used to check the adequacy of the model and of the variables associated with it.

3D surface and iso-contours plots were used to evaluate the combined effects of machining parameters on tool wear and surface roughness.

Finally, the multi-objective optimization of tool wear ( $VB$ ) and surface roughness ( $Ra$ ) was performed using the desirability function ( $DF$ ) approach. The following conclusions can be drawn from this study:

- ✓ The influence of each factor on the response results, such as tool wear and surface roughness, can be investigated by analysing the machining parameters using the RSM approach.
- ✓ The ANOVA table for tool flank wear showed that the cutting speed ( $Vc$ ) is the most influential parameter with a contribution of 16.28% compared to the other parameters. In addition, with contributions of 12.00%, 8.55% and 12.28% respectively, the interactions ( $Vc \times Vc$ ), ( $a_p \times Vc$ ) and ( $a_p \times f$ ) have a significant influence on the evolution of the  $VB$  flank wear.
- ✓ The ANOVA table for surface roughness showed that tool feed is the most significant parameter, followed by cutting speed and tool tip radii. In addition, feed rate had the greatest effect on tool flank wear (36.76%), followed by cutting speed and interaction ( $a_p \times r$ ), their contribution is 10.52% and 6.61% respectively.

On the basis of the multi-response optimization process, the optimum cutting variables for minimum tool flank wear with minimum surface roughness were a cutting depth of 0.1 mm, a cutting speed of 114.95 m/min, a feed rate of 0.11 mm/rev and a tool radius of 0.779 mm. The optimum values for tool flank wear and surface roughness are 0.096 mm and 0.402  $\mu\text{m}$ , respectively. The desired value is 0.915.

## References

1. Hasan, M. S.; Mazid, A. M.; Clegg, R. 2016. The basics of stellites in machining perspective, International Journal of Engineering Materials and Manufacture 1(2): 35-50.  
<https://doi.org/10.26776/ijemm.01.02.2016.01>.
2. Bagci, E.; Aykut, S. 2006. A study of Taguchi optimization method for identifying optimum surface roughness in CNC face milling of cobalt-based alloy (stellite 6), The International Journal of Advanced Manufacturing Technology 29: 940-947.

- <https://doi.org/10.1007/s00170-005-2616-y>.
3. **Aykut, Ş.; Gölcü, M.; Semiz, S.; Ergür, H.S.** 2007. Modeling of cutting forces as function of cutting parameters for face milling of satellite 6 using an artificial neural network, *Journal of Materials Processing Technology* 190: 199-203.  
<https://doi.org/10.1016/j.jmatprotec.2007.02.045>.
  4. **Folea, M.; Schlegel, D.; Lupulescu, N.-B.; PARV, L.** 2009. Modeling Surface Roughness in High Speed Milling: Cobalt Based Superalloy Case Study. In: *Proceedings of 1st International Conference on Manufacturing Engineering Quality Production System II*: 353-357.
  5. **Shao, H.; Li, L.; Liu, L. J.; Zhang, S. Z.** 2013. Study on machinability of a stellite alloy with uncoated and coated carbide tools in turning, *Journal of Manufacturing Processes* 15(4): 673-681.  
<https://doi.org/10.1016/j.jmapro.2013.10.001>
  6. **Zare Chavoshi, S.** 2013. Modelling of surface roughness in CNC face milling of alloy stellite 6, *International Journal of Computational Materials Science and Surface Engineering* 5(4): 304-321.  
<https://doi.org/10.1504/IJCMSSE.2013.059121>.
  7. **Ozturk, S.** 2014. Machinability of Stellite-6 Coatings with Ceramic Inserts and Tungsten Carbide Tools, *Arabian Journal for Science and Engineering* 39: 7375-7383.  
<https://doi.org/10.1007/s13369-014-1343-9>.
  8. **Bordin, A.; Bruschi, S.; Ghiotti, A.** 2014. The Effect of Cutting Speed and Feed Rate on the Surface Integrity in Dry Turning of CoCrMo Alloy, *Procedia CIRP*, 2nd CIRP Conference on Surface Integrity (CSI) 13: 219-224.  
<https://doi.org/10.1016/j.procir.2014.04.038>.
  9. **Sarikaya, M.; Güllü, A.** 2015. Multi-response optimization of minimum quantity lubrication parameters using Taguchi-based grey relational analysis in turning of difficult-to-cut alloy Haynes 25, *Journal of Cleaner Production* 91: 347-357.  
<https://doi.org/10.1016/j.jclepro.2014.12.020>.
  10. **Sarikaya, M.; Güllü, A.** 2015. Examining of Tool Wear in Cryogenic Machining of Cobalt-Based Haynes 25 Superalloy. *World Academy of Science, Engineering and Technology, International Journal of Chemical, Molecular, Nuclear, Materials and Metallurgical Engineering* 9(8): 911-915.
  11. **Sarikaya, M.; Yilmaz, V.; Güllü, A.** 2016. Analysis of cutting parameters and cooling/lubrication methods for sustainable machining in turning of Haynes 25 superalloy, *Journal of Cleaner Production* 133: 172-181.  
<https://doi.org/10.1016/j.jclepro.2016.05.122>.
  12. **Yingfei, G.; De Escalona, P. M.; Galloway, A.** 2017. Influence of cutting parameters and tool wear on the surface integrity of cobalt-based stellite 6 alloy when machined under a dry cutting environment, *Journal of Materials Engineering and Performance* 26(1): 312-326.  
<https://doi.org/10.1007/s11665-016-2438-0>.
  13. **Saidi, R.; Fathallah, B. B.; Mabrouki, T.; Belhadi, S.; Yallese, M. A.** 2019. Modeling and optimization of the turning parameters of cobalt alloy (Stellite 6) based on RSM and desirability function, *The International Journal of Advanced Manufacturing Technology* 100: 2945-2968.  
<https://doi.org/10.1007/s00170-018-2816-x>.
  14. **Saidi, R.; Fathallah, B. B.; Mabrouki, T.; Belhadi, S.; Yallese, M. A.** 2020. Prediction of Forces Components During the Turning Process of Stellite 6 Material Based on Artificial Neural Networks, in: Aifaoui, N., Affi, Z., Abbes, M.S., Walha, L., Haddar, M., Romdhane, L., Benamara, A., Chouchane, M., Chaari, F. (Eds.), *Design and Modeling of Mechanical Systems - IV, Lecture Notes in Mechanical Engineering*. Springer International Publishing, Cham, pp. 399-408.  
[https://doi.org/10.1007/978-3-030-27146-6\\_43](https://doi.org/10.1007/978-3-030-27146-6_43).
  15. **Bogajo, I. R.; Tangpronprasert, P.; Virulsri, C.; Keeratihattayakorn, S.; Arrazola, P. J.** 2020. A novel indirect cryogenic cooling system for improving surface finish and reducing cutting forces when turning ASTM F-1537 cobalt-chromium alloys, *The International Journal of Advanced Manufacturing Technology* 111: 1971-1989.  
<https://doi.org/10.1007/s00170-020-06193-x>.
  16. **Valíček, J.; Harničárová, M.; Řehoř, J.; Kušnerová, M.; Gombár, M.; Drbůl, M.; Šajgalík, M.; Filipenský, J.; Fulemová, J.; Vagaská, A.** 2020. Prediction of Cutting Parameters of HVOF-Sprayed Stellite 6, *Applied Sciences* 10(7): 2524.  
<https://doi.org/10.3390/app10072524>.
  17. **Andhare, A. B.; Kannathasan, K.; Funde, M.** 2021. Optimization of Machining Parameters for Turning of Haynes 25 Cobalt-Based Superalloy, in: Kalamkar, V.R., Monkova, K. (Eds.), *Advances in Mechanical Engineering, Lecture Notes in Mechanical Engineering*. Springer, Singapore, pp. 703-710.  
[https://doi.org/10.1007/978-981-15-3639-7\\_84](https://doi.org/10.1007/978-981-15-3639-7_84).
  18. **Benghersallah, M.; Boulanouar, L.; Coz, G. L.; Devillez, A.; Dudzinski, D.** 2010. Machinability of Stellite 6 hardfacing, *EPJ Web of Conferences* 6: 02001.  
<https://doi.org/10.1051/epjconf/20100602001>.
  19. **Hazir, E.; Ozcan, T.** 2019. Response Surface Methodology Integrated with Desirability Function and Genetic Algorithm Approach for the Optimization of CNC Machining Parameters, *Arabian Journal for Science and Engineering* 44: 2795-2809.  
<https://doi.org/10.1007/s13369-018-3559-6>.
  20. **Şap, S.; Usca, Ü. A.; Uzun, M.; Kuntoğlu, M.; Salur, E.; Pimenov, D. Y.** 2022. Investigation of the Effects of Cooling and Lubricating Strategies on Tribological Characteristics in Machining of Hybrid Composites, *Lubricants* 10(4): 63.  
<https://doi.org/10.3390/lubricants10040063>.
  21. **Değirmenci, Ü.; Usca, Ü. A.; Şap, S.** 2023. Machining characterization and optimization under different cooling/lubrication conditions of Al-4Gr hybrid composites fabricated by vacuum sintering, *Vacuum* 208: 111741.  
<https://doi.org/10.1016/j.vacuum.2022.111741>.
  22. **Tamil Alagan, N.; Zeman, P.; Hoier, P.; Beno, T.; Klement, U.** 2019. Investigation of micro-textured cutting tools used for face turning of alloy 718 with high-pressure cooling, *Journal of Manufacturing Processes* 37: 606-616.  
<https://doi.org/10.1016/j.jmapro.2018.12.023>.
  23. **Sivaiah, P.; Chakradhar, D.** 2019. Modeling and optimization of sustainable manufacturing process in machining of 17-4 PH stainless steel, *Measurement* 134: 142-152.  
<https://doi.org/10.1016/j.measurement.2018.10.067>.

24. **Meddour, I.; Yallese, M.A.; Bensouilah, H.; Khellaf, A.; Elbah, M.** 2018. Prediction of surface roughness and cutting forces using RSM, ANN, and NSGA-II in finish turning of AISI 4140 hardened steel with mixed ceramic tool, *The International Journal of Advanced Manufacturing Technology* 97: 1931-1949.  
<https://doi.org/10.1007/s00170-018-2026-6>
25. **Zaman, P. B.; Dhar, N. R.** 2020. Multi-objective Optimization of Double-Jet MQL System Parameters Meant for Enhancing the Turning Performance of Ti-6Al-4V Alloy, *Arabian Journal for Science and Engineering* 45: 9505-9526.  
<https://doi.org/10.1007/s13369-020-04806-x>
26. **Mia, M.; Khan, M. A.; Dhar, N. R.** 2017. Study of surface roughness and cutting forces using ANN, RSM, and ANOVA in turning of Ti-6Al-4V under cryogenic jets applied at flank and rake faces of coated WC tool, *The International Journal of Advanced Manufacturing Technology* 93: 975-991.  
<https://doi.org/10.1007/s00170-017-0566-9>.

R. Saidi, T. Mabrouki, B. Ben Fathallah, S. Belhadi, M. A. Yallese

# STUDY OF INSERT FLANK WEAR AND SURFACE ROUGHNESS EVOLUTIONS DURING TURNING OF STELLITE 6 BASED ON RSM AND DESIRABILITY APPROACHES

## S u m m a r y

In this research, turning experiments on Co-Cr-Mo, cobalt-based alloy Stellite 6) were carried out to examine the effect of four machining factors (tool tip radii, feed rate, cutting depth and cutting speed) on insert flank wear and surface roughness. On the basis of a design Taguchi plan ( $L^{18}$ ), the experiments were conducted. The response surface methodology (RSM) was employed to develop mathematical modelling of flank wear and surface roughness evolutions. The contribution of each individual parameter to process responses was assessed using ANOVA analysis. Predicted models in relationship with flank wear and surface roughness evolutions were obtained from the regression equation. These models show good correlations with experimental results. A maximum error of 13.82% and 10.90% of flank wear and surface roughness was observed between simulated and experimental results, respectively. The optimization of processing parameters was investigated in order to achieve both the minimum values of flank wear band and surface roughness.

**Keywords:** machining, ANOVA: RSM, Stellite 6, flank wear, surface roughness.

Received February 27, 2025

Accepted August 22, 2025



This article is an Open Access article distributed under the terms and conditions of the Creative Commons Attribution 4.0 (CC BY 4.0) License (<http://creativecommons.org/licenses/by/4.0/>).